Gem-diols-type intermediate of ketone activation on sn-β zeolite as studied by solid-state nmr spectroscopy

Guodong Qi, Yueying Chu, Qiang Wang, Xingxing Wang, Yi Li, Julien Trebosc, Olivier Lafon, Jun Xu, Feng Deng

Gem-diols-type intermediate of Ketone Activation on Sn-β Zeolite as Studied by Solid-state NMR Spectroscopy

Guodong Qi†, Yueying Chu†, Qiang Wang, Xingxing Wang, Yi Li, Julien Trébosc, Olivier Lafon, Jun Xu* and Feng Deng

[*] Dr. G.D. Qi, Dr. Y.Y. Chu, Dr. Q. Wang, Prof. J. Xu and Prof. F. Deng
National Centre for Magnetic Resonance in Wuhan, State Key Laboratory of Magnetic Resonance and Atomic and Molecular Physics, Key Laboratory of Magnetic Resonance in Biological Systems, Wuhan Institute of Physics and Mathematics, Innovation Academy for Precision Measurement Science and Technology, Chinese Academy of Sciences, Wuhan 430071, China. University of Chinese Academy of Sciences, Beijing 100049, China.
E-mail: xujun@wipm.ac.cn
†Equally contribute to this work
Prof. J. Xu
Wuhan National Laboratory for Optoelectronics, Huazhong University of Science and Technology, Wuhan 430074, China.
X.X. Wang, Prof. Y. Li
State Key Laboratory of Inorganic Synthesis and Preparative Chemistry, College of Chemistry, Jilin University, 2699 Qianjin Street, Changchun 130012, China
Prof. Y. Li
International Center of Future Science, Jilin University, Changchun 130012, China
Dr. J. Trébosc
Univ. Lille, CNRS, INRA, Centrale Lille, ENSCL, Univ. Artois, FR 2638 - IMEC - Institut Michel-Eugène Chevreul, F-59000 Lille, France
Prof. O. Lafon
Univ. Lille, CNRS, Centrale Lille, Univ. Artois, UMR 8181 – UCCS – Unité de Catalyse et Chimie du Solide, F-59000 Lille, France
Institut Universitaire de France, 75231 Paris, France

Supporting information for this article is given via a link at the end of the document.

Abstract: Lewis acid zeolites have found an increasing application in the field of biomass conversion, in which the selective transformation of carbonyl-containing molecule is of particular importance due to its relevance in organic synthesis. Mechanistic insight into the activation of carbonyl group on Lewis acid sites is challenging and critical for the understanding of the catalytic process, which requires the identification of reaction intermediates. Here we report the observation of a stable surface *gem*-diols-type species in the activation of acetone on Sn-β zeolite. ^{13}C, ^{119}Sn and ^{13}C-^{119}Sn double-resonance NMR spectroscopies demonstrate that only the open Sn site ($(SiO)_3Sn$-OH) on Sn-β is responsible for the formation of the surface species. ^{13}C MAS NMR experiments together with density functional theory calculations suggest that the *gem*-diols-type species exhibits high reactivity and can serve as an active intermediate in the Meerwein–Ponndorf–Verley-Oppenauer (MPVO) reaction of acetone with cyclohexanol. The *gem*-diols-type species offers an energy-preferable pathway for the direct carbon-to-carbon hydrogen transfer between ketone and alcohol. The results provide new insights into the transformation of carbonyl-containing molecules catalyzed by Lewis acid zeolites.

Introduction

The catalytic conversion of renewable biomass has particularly attracted a lot of attention because it provides a viable route for the production of biofuels or chemicals, while reducing the use of fossil resources and mitigating global warming[1]. Conversion of biomass feedstock consists in the production of low-weight intermediates that feature multiform oxygenic groups, such as carbonyl, hydroxyl and ether groups and further upgrading of these materials to fuel components or chemical intermediates. Because of the high oxygen content and the intrinsic reactivity of the oxygenic groups, the transformation of biomass-derived materials in liquid-phase under mild reaction conditions is preferred. Lewis acid zeolites and zeo-type materials are promising catalysts in the field of biomass valorization[2], such as conversion of

glycerol and sugars to high-value chemicals. Specifically, metal (e.g., Sn, Ti, Zr, Ta, etc.) modified zeolites are intensively studied due to their hydrophobic nature and distinct activity for converting a number of oxygenated molecules under mild condition[3].

Carbonyl groups exist in a wide range of biomass-derived materials. For example, ketones, carboxylic acids and aldehydes are the main components in bio-oil derived from biomass pyrolysis[4]. The conversion of carbonyl-containing molecules often involves deoxygenation and rearrangement of C-C bonds. The Meerwein–Ponndorf–Verley carbonyl reduction of aldehydes and ketones and the complementary Oppenauer oxidation of alcohol (MPVO) is an important reaction in the selective reduction of carbonyl-containing compounds with secondary alcohols[5], which offers a conceptually ideal approach for intra- or inter-molecular hydrodeoxygenation of biomass-derived ketones without consumption of hydrogen[3f, 6]. The MPVO reaction entails the presence of Lewis acid metal centers in the catalyst[7]. Among the widely explored solid Lewis acids[8], Sn incorporated Beta (Sn-β) zeolite is demonstrated to be the most active and selective catalyst[3f, 3h, 6a, 6b].. The superior performance of Sn-β zeolite is due to the generation of Lewis acidic Sn sites in the hydrophobic zeolite channels[9].

Considerable efforts have been devoted to determine the nature of Sn active catalytic site[9a, 10], which is particularly challenging under reaction conditions due to the variation of metal site speciation. Partially hydrolyzed Sn site (open site, $(SiO)_3Sn$-OH), fully coordinated (closed site, $(SiO)_4Sn$) Sn site and extra-framework SnO_2 particles are supposed to be formed on Sn-β zeolites depending on the preparation method. It was indicated in MPVO reaction the initial reaction rate linearly correlated with the amount of open Sn site[11]. As indicated by Na^+, NH_3 and pyridine poisoning experiments, the open site exhibits a higher reactivity in the isomerization of glucose[10d, 12]. Though the extra-framework SnO_2 species is not often considered as active sites[13], the work by Davis and co-workers concluded that isomerization of glucose to fructose occurs on both framework and extra-framework Sn sites encaged in the hydrophobic channels of Sn-β zeolite[10a]. Understanding of the metal speciation and further controlling their distributions is important to gain insight into the catalytic behavior of Sn-β zeolite and the underlying reaction mechanism.

The activation of carbonyl-containing molecules on Sn-β zeolites has been widely attributed to a coordination of the carbonyl group to the Sn site. For Baeyer-Villiger (BV) oxidation that allows the transformation of ketones into esters or lactones, the Sn site activates the carbonyl group which favors the attack by nucleophilic hydrogen peroxide[14].. In the theoretically predicted pathway of MPVO reaction, the key step is the adsorption of ketone and alcohol to the framework Sn site, forming a six-membered cyclic transition state which facilitates the hydride transfer from the alcohol to the carbonyl group[11]. It is well-recognized that the formation of carbonyl complex with Sn site enables the polarization of carbonyl group with increased electrophilicity. The coordination of carbonyl groups could exist in different modes, which influence the reactivity of the carbonyl complex[7]. Although many reaction mechanisms involving carbonyl groups have been proposed on Sn-β zeolite, the activation of carbonyl group has not been experimentally explored. Insight into the nature of the carbonyl group derived intermediates is critical for a better understanding of the active site on Sn-β and the organic reactions that involve carbonyl groups.

Solid-state NMR is a powerful tool in the field of heterogeneous catalysis for characterizing the active sites and reaction intermediates on zeolites[15]. In our previous work, the open Sn site was selectively observed and quantitatively determined on hydrothermally synthesized Sn-β zeolite by proton-detected $^1H/^{119}Sn$ solid-state NMR correlation spectroscopy[10f]. Reversible transformation between open and closed Sn sites

occurs upon hydration and dehydration treatment of the sample, which allows for a facile control of the generation of the two types sites on Sn-β zeolite. Here, we establish an experimental understanding of the activation of carbonyl groups in MPVO reaction over Sn-β zeolite, which is corroborated by theoretical calculations. Acetone and cyclohexanol are selected for the reaction, since they are often used as model substrates in theoretical studies[11, 16]. By using ^{13}C, ^{119}Sn and ^{13}C-^{119}Sn double-resonance MAS NMR techniques, the formation of a surface *gem*-diols-type species is identified in the activation of acetone on the open Sn site via –OH nucleophilic addition on carbonyl group. The *gem*-diols-type species plays an intermediate role in the reaction of acetone with cyclohexanol via the MPVO process, which facilitates the six-membered carbon-to-carbon hydrogen transfer between ketone and alcohol.

Results and Discussion

Identification of *gem*-diols-type species on Sn-β zeolite.

All Sn-β zeolites with 1.2 wt.% of Sn were synthesized by direct hydrothermal method[14a] (see details in the supporting information). A pure silica β zeolite (denoted as Si-β) was also synthesized with the same method used for comparison. For solid-state NMR analysis, ^{119}Sn-enriched ^{119}Sn-β zeolite was prepared by using ^{119}Sn metal foil (with 97.4 % ^{119}Sn abundance) as the Sn source. A detailed physical characterizations including X-ray powder diffraction (XRD), scanning electron microscopy with energy dispersive spectroscopy (TEM-EDS), and diffuse reflectance ultraviolet-visible spectroscopy (DR-UV-vis) were conducted in our previous work[10f], which showed that all the obtained samples were well crystallized with the topological structure of zeolite β and the metal Sn atoms were homogeneously incorporated into the zeolite framework. The activation of acetone on Sn-β zeolite was monitored by solid-state ^{13}C NMR spectroscopy at room temperature in order to avoid side reactions. Figure 1a and b shows the $^{1}H \rightarrow ^{13}C$ cross-polarization under magic-angle spinning (CP MAS) spectra obtained from [2-^{13}C]-acetone adsorption on Sn-β zeolite dehydrated at 393 K. We previously showed that both open and closed Sn sites were generated, with the amount of open Sn site being 17% of total Sn content on the zeolite. Two signals at 76 and 229 ppm were observed at low [2-^{13}C]-acetone loading (30 μmol/g) (Figure 1a), where the mole ratio of acetone to Sn atoms is approximately 0.3. Increasing the loading of [2-^{13}C]-acetone to 100 μmol/g (with the mole ratio of acetone to Sn atom being about 1) leads to two new signals at 217 ppm and 29 ppm (Figure 1b). In a control experiment, the physisorbed [2-^{13}C]-acetone molecules on Si-β zeolite channels produce ^{13}C signals of carbonyl carbon at 206 ppm and of methyl group at 29 ppm (Figure S1). Therefore, the observed deshielding signals at 217 and 229 ppm in Sn-β zeolite can be assigned to acetone adsorbed on different Lewis acidic Sn sites[17]. The 76 ppm signal in the region of chemical shift for single carbon-oxygen bond should be produced by the interaction of carbonyl carbon of [2-^{13}C]-acetone with Sn site, similar to the adsorbed alcohol or surface alkoxide[18].

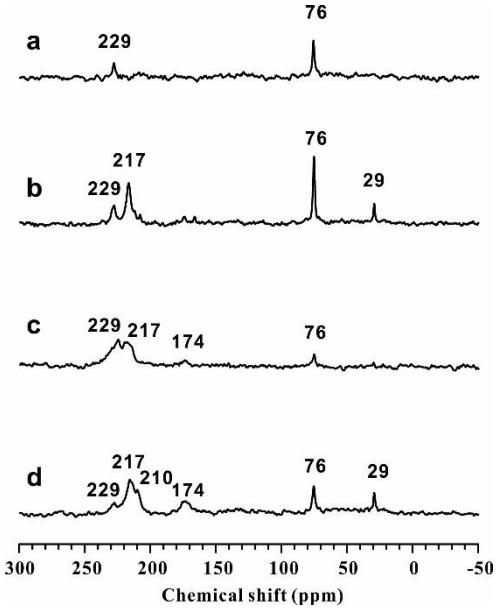

Figure 1. $^{1}H \rightarrow {}^{13}C$ CP MAS NMR spectra of (a) 30 μmol/g and (b) 100 μmol/g of [2-^{13}C]-acetone adsorbed on Sn-β zeolite dehydrated at 393 K, (c) 30 μmol/g and (d) 100 μmol/g of [2-^{13}C]-acetone adsorbed on Sn-β zeolite dehydrated at 673 K.

To explore the interaction of alcohol with Sn site, ^{13}C-labelled [2-^{13}C]-*iso*-propanol was deliberately adsorbed on Sn-β zeolite. As shown in the ^{13}C NMR spectrum (Figure S2), both the physisorbed *iso*-propanol and *iso*-propyl alkoxy species generated by the dehydration of *iso*-propanol are observed

on the zeolite, which produce methenyl signals at 69 and 72 ppm, respectively. In organic chemistry synthesis, the attack of oxygen containing nucleophiles (e.g., H_2O and OH^-) on the carbonyl group of aldehydes and ketones usually leads to an unstable *gem*-diols structure[19]. Recently, the stable *gem*-diols-type species were identified in carbonyl-containing organic compounds, such as formylpyridine[20] and imidazole[21] derivatives, which have ^{13}C chemical shift fingerprints in the range of 70~100 ppm. Thus, it is most likely that the -OH group of the open Sn site is involved in the nucleophilic attack on the carbonyl group of adsorbed [2-^{13}C]-acetone producing a *gem*-diols-type species, which probably resonates at 76 ppm in the ^{13}C NMR spectrum.

We have shown that the open Sn site can be transformed into closed site upon the dehydration treatment of the sample at temperature up to 673 K[10f]. In order to differentiate the two types of Sn sites for the adsorption of acetone and the formation of the *gem*-diols-type species, the activation of acetone was also performed on Sn-β zeolite dehydrated at higher temperature of 673 K, where the closed Sn sites are predominant. As shown in Figure 1c and d, the 76 ppm signal was remarkably reduced on the samples with different acetone loadings compared to that in Figure 1a and 1b, indicating that the open Sn site should be responsible for the formation of the *gem*-diols-type species. The activation of acetone occurring at room temperature points to a high activity of the open Sn site toward the carbonyl group. The 217 and 229 ppm signals are still observable, which can thus be attributed to the adsorbed acetone on the closed Sn sites. These adsorbed acetones cannot be directly activated at this condition. In addition to the physisorbed acetone at ca. 210 ppm, the new signal at 174 ppm is due to formate species[22], which could be due to the oxidation of acetone molecules on the highly dehydrated sample.

The coordination of the *gem*-diols-type group to the Sn site was further explored by solid-state NMR experiment (Figure 2). In particular, the $^{13}C\{^{119}Sn\}$ symmetry-based rotational-echo double-resonance (S-REDOR) method[15b, 23] (Figure S4) was utilized, which allows for detection of the dipolar interaction

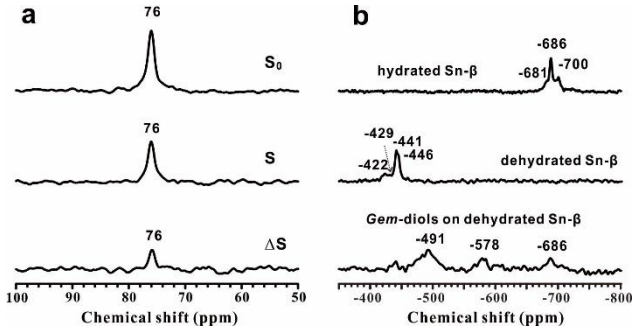

Figure 2. (a) $^{13}C\{^{119}Sn\}$ S-REDOR S0, S and ΔS spectra of 100 μmol/g of [2-^{13}C]-acetone adsorbed on ^{119}Sn-β dehydrated at 393 K probing the spatial proximity between tin atoms and *gem*-diols-type group. (b) ^{119}Sn MAS NMR spectra of hydrated ^{119}Sn-β (top), dehydrated ^{119}Sn-β before (middle) and after (bottom) adsorption of 100 μmol/g of [2-^{13}C]-acetone to produce *gem*-diols.

between the ^{13}C atom in the *gem*-diols-type group and the proximate ^{119}Sn atom in Sn-β framework. For the Sn site bound to *gem*-diols-type species, the associated ^{13}C signal will be modulated by the ^{13}C-^{119}Sn dipolar interaction under ^{119}Sn irradiation in the $^{13}C\{^{119}Sn\}$ S-REDOR experiment. The activation of [2-^{13}C]-acetone was performed on ^{119}Sn-enriched ^{119}Sn-β at the same condition as that of Figure 1b. As shown in Figure 2a, the dephasing under ^{13}C-^{119}Sn dipolar interaction was estimated by calculating the difference spectrum ($\Delta S = S_0 - S$), obtained by subtracting the ^{13}C NMR spectrum with ^{119}Sn irradiation (S) from that without ^{119}Sn irradiation (S_0). The 76 ppm signal is obviously observed in the difference spectrum (ΔS), providing compelling evidence on the spatial proximity/interaction between the *gem*-diols-type group and the open Sn site in ^{119}Sn-β.

The formation of the Sn bound species is also reflected in the ^{119}Sn MAS NMR spectra (Figure 2b). The three signals at -681, −686 and −700 ppm observed on the hydrated Sn-β belong to octahedral Sn sites formed by adsorption of water molecules on tetrahedral Sn sites[10a, 14a]. In comparison, the tetrahedral Sn sites produce a set of signals at −422, −429, −441 and −446 ppm on Sn-β dehydrated at 393 K. After acetone was adsorbed on ^{119}Sn-β dehydrated at 393 K, pentahedral Sn sites at −578 ppm and hexahedral Sn sites at -686 ppm are observed due to the coordination of one or two acetone molecules to the tetrahedral Sn sites respectively[24]. Interestingly, a broad and upper-field signal appeared at −491 ppm. Since the *gem*-diols-type species was generated on the sample, this new signal can be ascribed to the open Sn sites bound to *gem*-diols group. The distribution of local environment induced by the bound organic group leads to the line broadening of the ^{119}Sn signal.

In order to understand the generation of the observed *gem*-diols species and gain information on its structure, density functional theory (DFT) calculations were performed on the activation of acetone on the open Sn site. A periodic model of the open Sn site in Sn-β zeolite was used for the theoretical analysis, in which the thermodynamically preferred open Sn site was located at T9 lattice position of zeolite framework[25] (Figure S3). Figure 3 shows the optimized local structures and the corresponding energy profile of elementary steps in the formation of the *gem*-diols species on the open Sn site. The adsorption

of acetone on the open Sn site (Ace) releases an energy of 43.5 kcal/mol. The polarized carbonyl group coordinated to Sn atom becomes

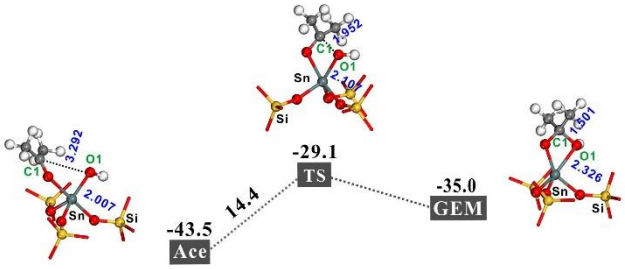

Figure 3. DFT optimized local structures and reaction profile for the formation of *gem*-diols species on open Sn site. The energy is provided in kcal/mol, relative to the sum of the energy for gas ketone and isolated Sn-β zeolite. The main interatomic distances are given in Å.

susceptible to nucleophilic attack at the C atom by the spatially proximate -OH group associated with the open Sn site (C-O distance being 3.292 Å). The bonding of the -OH group to the carbonyl carbon atom produces the surface *gem*-diols-type species (GEM) with an energy barrier of 14.4 kcal/mol and reaction energy of 8.5 kcal/mol. This low energy barrier is consistent with the experimental observation of the acetone activation on the open Sn site. A neighboring Si-OH group was also considered in the optimized structure (Figure S3), which was found to have no influence on the activation of acetone.

Taking above results together, it can be confirmed that acetone adsorbed on the open Sn site is readily attacked by the nearby Sn-OH group via the nucleophilic addition producing the surface *gem*-diols-type species. In analogue to multifunctional organometallic compounds[26], the gem-diols-type group does not exist as a free species but in form of metal complex. This indicates the critical role of the active open Sn site in stabilizing the gem-diols-type species in Sn-β zeolite.

Reactivity of *gem*-diols-type species.

The observation of the stable g*em*-diols-type group on Sn-β allows us to probe its reactivity in catalytic reactions. The reduction of acetone with cyclohexanol via MPVO process was used as the model reaction. The high yields and product selectivity of MPVO reaction would facilitate the species determination by NMR experiments. Cyclohexanol in natural abundance was introduced onto Sn-β on which the *gem*-diols-type species was pre-produced by the adsorption of [2-^{13}C]-acetone. The Sn-β samples were dehydrated at different temperatures to control the amount of both open sites and *gem*-diols-type species. The reactions were performed at room temperature to avoid side reactions. The loading of cyclohexanol were varied. As shown in the ^{1}H→^{13}C CP MAS NMR spectrum of Sn-β dehydrated at 393 K (Figure 4a), the *gem*-diols-type species at 76 ppm was notably reduced after introducing a small amount of cyclohexanol (100 μmol/g) compared to that observed in Figure 1b. The concomitant appearance of 72 ppm signal is ascribed to

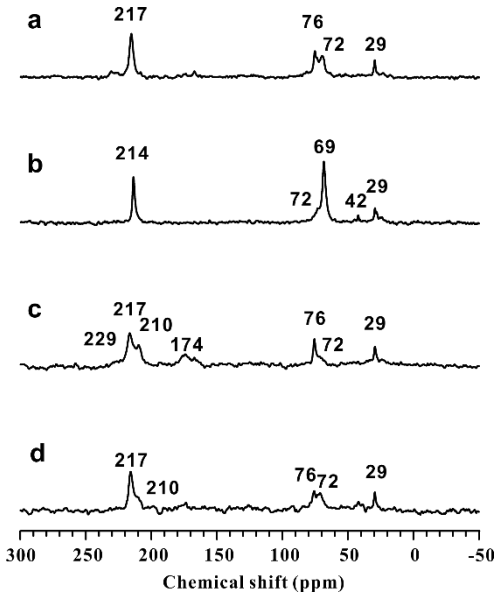

Figure 4. $^{1}H \rightarrow ^{13}C$ CP MAS NMR spectra of (a) 100 μmol/g and (b) 300 μmol/g of isotopically unmodified cyclohexanol adsorbed on Sn-β zeolite dehydrated at 393 K, where 100 μmol/g of [2-^{13}C]-acetone was pre-adsorbed as well as (c) 100 μmol/g and (d) 300 μmol/g of isotopically unmodified cyclohexanol adsorbed on Sn-β zeolite dehydrated at 673 K, where 100 μmol/g of [2-^{13}C]-acetone was pre-adsorbed.

iso-propyl alkoxy species similar to that produced by the adsorption of *iso*-propanol on Sn-β zeolite (Figure S2), resulting from the transformation of the gem-diols-type species. Increasing the loading of cyclohexanol (up to 300 μmol/g) leads to a further decline of the gem-diols-type species (76 ppm) (Figure 4b). Meantime, a decrease of isopropyl alkoxy species (72 ppm) is also evident. In addition, a new signal appears at 69 ppm, indicating the formation of *iso*-propanol molecule via the reaction of *iso*-propyl alkoxy species with water molecules. This suggests a consecutive reduction of the *gem*-diols-type species by cyclohexanol producing water. Note that a weak signal appears at 42 ppm as well, which can be assigned to the methylene ^{13}C atom on the ring of cyclohexanone (Figure 4b and Figure S5). The formation of *iso*-propanol and cyclohexanone demonstrates that the MPVO reaction proceeds on Sn-β.

The reactions were also carried out on the highly dehydrated Sn-β at 673 K (Figure 4c and d), on which the *gem*-diols-type species is markedly reduced due to the decrease of the open Sn site. The weak signal observed at 72 ppm indicates that only a small amount of *iso*-propyl alkoxy species was produced, while *iso*-propanol molecule (69 ppm) can be hardly observed, even at a higher loading of cyclohexanol (300 μmol/g). This indicates that the MPVO reaction is very limited on the highly dehydrated Sn-β due to the unfavorable formation of the *gem*-diols-type species. It may therefore be conjectured from these observations that the *gem*-diols-type species acts as the active intermediate in the MPVO reaction of ketones and alcohols.

Role of *gem*-diols-type species in MPVO reaction

The role of *gem*-diols-type species was further studied in the MPVO reaction. Direct hydrogen transfer and hydridic route have been proposed for the MPVO reaction in the literature[27] (Figure S6). To get direct information on the reaction route on Sn-β, an isotope tracer experiment was performed on the reaction of cyclohexanone and [2-^{2}H]-*iso*-propanol, which is the reverse of MPVO reaction of cyclohexanol with

acetone, the products were analyzed by liquid-state ^{13}C NMR (Figure S7). The spectra provides strong evidence that the deuterium atom at the C-2 position of [2-^{2}H]-*iso*-propanol reactant moved onto the C-1 position of cyclohexanol product, unambiguously demonstrating that the MPVO reaction on Sn-β zeolite undergoes a direct carbon-to-carbon hydrogen transfer route, in agreement with previous hypothesis[11, 27a, 28].

The direct carbon-to-carbon hydrogen transfer route is generally supposed to proceed through a six-membered cyclic transition state composed of adsorbed alcohol and ketone coordinated to the Lewis metal center (Figure S6a)[16]. Due to the lack of insight into the activation of reactant, the exact process leading to the carbon-to-carbon hydrogen transfer remains not well understood. Our above experimental results show that the activation of acetone produces a surface *gem*-diols-type species stabilized on the open Sn site, which acts as an intermediate in the MPVO on Sn-β zeolite. On the basis of our observation, a full catalytic cycle consisting of 8 steps is proposed for the reaction of ketone with cyclohexanol on Sn-β zeolite (Scheme 1). The pathway can be grouped into 4 parts: adsorption of acetone on open Sn site and formation of GEM intermediate in part A (steps 1-2), coordination of cyclohexanol to the Sn site forming a co-adsorbed complex (Co-ADS) in part B (steps 3-4), direct hydrogen transfer occurring via a six-membered cyclic transition state followed by formation of adsorbed cyclohexanone and isopropyl alkoxy species on the Sn site in part C (steps 5-6), and Part D (steps 7-8) composed of desorption of cyclohexanone and recovery of the open Sn site by hydrolysis of isopropyl alkoxy species to alcohol.

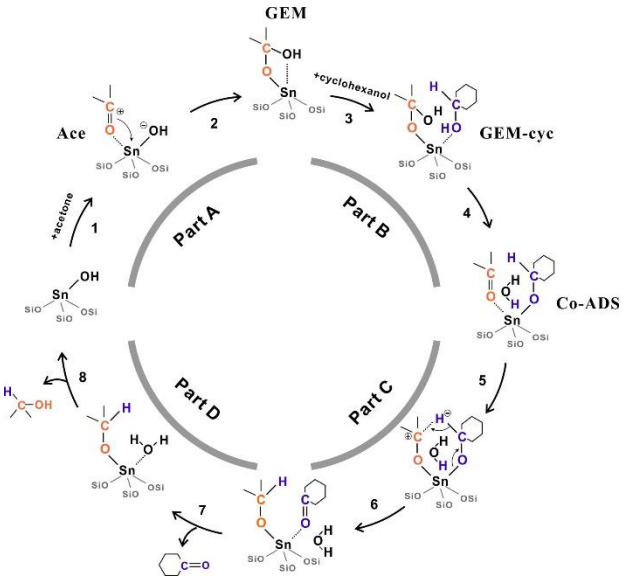

Scheme 1. Proposed catalytic cycle for the reaction between acetone and cyclohexanol on Sn-β zeolite.

DFT calculations were performed on the elementary steps with focus on part B to gain mechanistic insight into the reaction of the *gem*-diols-type species toward the formation of the Co-ADS complex. Figure 5 shows the optimized local structures and the corresponding reaction profile of elementary steps (steps 3-4). We have shown the facile formation of the GEM (Figure 2), starting from which a GEM-cyc adsorption state can be readily formed by adsorption of a cyclohexanol molecule on the open

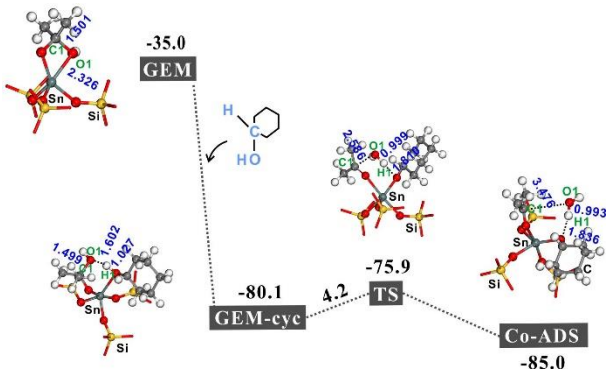

Figure 5. DFT optimized local structures and reaction profile for the formation of Co-ADS adsorption state from GEM. The energy is provided in kcal/mol, relative to the sum of the energy for gas acetone, cyclohexanol molecules and isolated Sn-β zeolite. The main interatomic distances are provided in Å.

Sn site with a notably exothermic process (-45.1 kcal/mol). A subsequent deprotonation of the adsorbed cyclohexanol by the neighboring hydroxyl group in the GEM proceeds with an activation barrier of 4.2 kcal/mol, resulting in the formation of co-adsorbed ketone and alkoxy species (Co-ADS). The low activation barrier is consistent with the above experimentally observed high reactivity of GEM. The subsequent production of isopropanol and cyclohexanone involving a six-membered cyclic transition state (part C and D) follows the similar steps as described in previous theoretical studies of the MPVO reaction[11, 16].

The co-adsorption of ketone and alcohol on the open Sn site was proposed for the formation of the Co-ADS complex in a previous computational study[11]. The similar process for acetone and cyclohexanol was analyzed by DFT calculations for comparison. The optimized structures for the co-adsorption pathway and calculated reaction profile are given in Figure S8. The adsorption energies (E_{ads}), activation energies (E_a) and reaction energies (E_r) are listed in Table 1, in which the data obtained from Figure 5 are included. In all respects, the GEM intermediate pathway is both thermodynamically and kinetically

Table 1. Calculated energies (in kcal/mol) for the GEM intermediate and Co-adsorption routes toward Co-ADS complex depicted in Figure 5 and Figure S8.

Pathway	E_{ads}	Deprotonation	
		E_a	E_r
GEM intermediate	−45.1	4.2	−4.9
Co-adsorption	−40.7	5.6	−0.8

E_{ads}: cyclohexanol adsorption energy, E_a: activation energy for the formation of Co-ADS complex, E_r: reaction energy ($E_{Co\text{-}ADS}$−$E_{GEM/Ace\text{-}cyc}$).

preferred over the co-adsorption route as it provides a stronger cyclohexanol adsorption and lower activation energy for the following deprotonation process along with a more stabilized Co-ADS complex (more negative E_r value). Thus, it can be concluded from the experimental and DFT results that the GEM is formed as an active intermediate in the MPVO reaction on Sn-β zeolite. The role of the GEM intermediate is twofold. First, the formation of GEM enhances the adsorption capacity of the Sn site for alcohol. Second, it provides a favorable pathway for the activation of the adsorbed alcohol, enabling a facile formation of the six-membered cyclic transition state for hydrogen transfer (part C in Scheme 1).

Conclusion

The activation of ketone and its transformation on Sn-β was investigated by combined solid-state NMR experiments and DFT calculations. Acetone can be readily activated on partially dehydrated Sn-β at room temperature, where the open Sn site acts as the active site. The *gem*-diols-type species is for the first time observed and identified as the stable surface species bound to the open Sn site by $^{13}C\{^{119}Sn\}$ double-resonance NMR experiments. DFT calculations revealed that the polarized carbonyl group of acetone coordinated to Sn atom is susceptible to nucleophilic attack by the spatially proximate Sn-OH group, responsible for the formation of the *gem*-diols-type species. The surface *gem*-diols-type species shows high reactivity towards cyclohexanol, which leads to a facile formation of *iso*-propanol and cyclohexanone via the MPVO process. Although the direct carbon-to-carbon hydrogen transfer has been well-recognized as the key step in the MPVO reaction, our experiments and DFT calculations demonstrate that the *gem*-diols-type species can serve as an active intermediate, providing an energy-favorable route for the direct hydrogen transfer reaction. The results presented herein will be helpful for understanding the reaction of ketone catalyzed by Lewis acid zeolite and the carbonyl chemistry.

Acknowledgements

This work was supported by the National Natural Science Foundation of China (Grants 21872170, U1932218, 22061130202, 21733013, 91745111), Key projects of international partnership plan for foreign cooperation (112942KYSB20180009), key program for frontier science of the Chinese Academy of Sciences (QYZDB-SSW-SLH027) and Hubei Provincial Natural Science Foundation (2017CFA032).

Conflict of interest

The authors declare no conflict of interest.

Keywords: Ketone • Intermediate • Zeolites • Carbonyl group • Solid-state NMR

[1] a) G. W. Huber, S. Iborra, A. Corma, *Chem. Rev.* **2006**, *106*, 4044-4098; b) A. J. Ragauskas, C. K. Williams, B. H. Davison, G. Britovsek, J. Cairney, C. A. Eckert, W. J. Frederick, J. P. Hallett, D. J. Leak, C. L. Liotta, J. R. Mielenz, R. Murphy, R. Templer, T. Tschaplinski, *Science* **2006**, *311*, 484-489; c) P. Gallezot, *Chem. Soc. Rev.* **2012**, *41*, 1538-1558; d) M. Besson, P. Gallezot, C. Pinel, *Chem. Rev.* **2014**, *114*, 1827-1870.

[2] a) E. Taarning, C. M. Osmundsen, X. B. Yang, B. Voss, S. I. Andersen, C. H. Christensen, *Energy Environ. Sci.* **2011**, *4*, 793-804; b) T. Ennaert, J. Van Aelst, J. Dijkmans, R. De Clercq, W. Schutyser, M. Dusselier, D. Verboekend, B. F. Sels, *Chem. Soc. Rev.* **2016**, *45*, 584-611; c) Y. Li, L. Li, J. Yu, *Chem* **2017**, *3*, 928-949; d) W. Luo, W. Cao, P. C. A. Bruijnincx, L. Lin, A. Wang, T. Zhang, *Green Chem.* **2019**, *21*, 3744-3768.

[3] a) A. Corma, H. Garcia, *Chem. Rev.* **2002**, *102*, 3837-3892; b) D. Kubicka, I. Kubickova, J. Cejka, *Catal. Rev.* **2013**, *55*, 1-78; c) P. Y. Dapsens, C. Mondelli, J. Perez-Ramirez, *Chem. Soc. Rev.* **2015**, *44*, 7025-7043; d) H. Y. Luo, J. D. Lewis, Y. Román-Leshkov, *Annu. Rev. Chem. Biomol. Eng.* **2016**, *7*, 663-692; e) V. L. Sushkevich, Ivanova, II, S. Tolborg, E. Taarning, *J. Catal.* **2014**, *316*, 121-129; f) G. Li, W. Jiao, Z. Sun, Y. Zhao, Z. Shi, Y. Yan, L. Feng, Y. Zhang, Y. Tang, *ACS Sustain. Chem. Eng.* **2018**, *6*, 4316-4320; g) S. Van de Vyver, C. Odermatt, K. Romero, T. Prasomsri, Y. Román-Leshkov, *ACS Catal.* **2015**, *5*, 972-977; h) M. Moliner, Y. Román-Leshkov, M. E. Davis, *Proc. Natl. Acad. Sci. USA* **2010**, *107*, 6164-6168; i) G. W. Huber, J. N. Chheda, C. J. Barrett, J. A. Dumesic, *Science* **2005**, *308*, 1446-1450; j) Y. Román-Leshkov, J. N. Chheda, J. A. Dumesic, *Science* **2006**, *312*, 1933-1937; k) L. D. Schmidt, P. J. Dauenhauer, *Nature* **2007**, *447*, 914-915; l) Y. Roman-Leshkov, C. J. Barrett, Z. Y. Liu, J. A. Dumesic, *Nature* **2007**, *447*, 982-985; m) M. Xu, W. Wang, M. Hunger, *Chem. Commun.* **2003**, 722-723.

[4] J. Huang, W. Long, P. K. Agrawal, C. W. Jones, *J. Phys. Chem. C* **2009**, *113*, 16702-16710.

[5] a) C. F. de Graauw, J. A. Peters, H. van Bekkum, J. Huskens, *Synthesis* **1994**, *1994*, 1007-1017; b) M. Schroeter, *Synthetic. Commun.* **2005**, *35*, 2203-2212.

[6] a) M. J. Gilkey, B. Xu, *ACS Catal.* **2016**, *6*, 1420-1436; b) S. Chen, R. Wojcieszak, F. Dumeignil, E. Marceau, S. Royer, *Chem. Rev.* **2018**, *118*, 11023-11117; c) R. López-Asensio, C. P. Jiménez Gómez, C. García Sancho, R. Moreno-Tost, J. A. Cecilia, P. Maireles-Torres, *Int. J. Mol. Sci.* **2019**, *20*, 828.

[7] Y. Román-Leshkov, M. E. Davis, *ACS Catal.* **2011**, *1*, 1566-1580.

[8] a) F. Wang, N. Ta, W. Shen, *Appl. Catal. A-gen.* **2014**, *475*, 76-81; b) P. Panagiotopoulou, N. Martin, D. G. Vlachos, *Chemsuschem* **2015**, *8*, 2046-2054; c) E. J. Creyghton, S. D. Ganeshie, R. S. Downing, H. van Bekkum, *J. Mol. Catal. A-chem.* **1997**, *115*, 457-472.

[9] a) S. R. Bare, S. D. Kelly, W. Sinkler, J. J. Low, F. S. Modica, S. Valencia, A. Corma, L. T. Nemeth, *J. Am. Chem. Soc.* **2005**, *127*, 12924-12932; b) G. Yang, L. J. Zhou, X. W. Han, *J. Mol. Catal. A-chem.* **2012**, *363*, 371-379.

[10] a) R. Bermejo-Deval, R. Gounder, M. E. Davis, *ACS Catal.* **2012**, *2*, 2705-2713; b) W. R. Gunther, V. K. Michaelis, M. A. Caporini, R. G. Griffin, Y. Román-Leshkov, *J. Am. Chem. Soc.* **2014**, *136*, 6219-6222; c) P. Wolf, M. Valla, A. J. Rossini, A. Comas-Vives, F. Nunez-Zarur, B. Malaman, A. Lesage, L. Emsley, C. Coperet, I. Hermans, *Angew. Chem. Int. Ed.* **2014**, *53*, 10179-10183; d) J. W. Harris, M. J. Cordon, J. R. Di Iorio, J. C. Vega-Vila, F. H. Ribeiro, R. Gounder, *J. Catal.* **2016**, *335*, 141-154; e) Y. G. Kolyagin, A. V. Yakimov, S. Tolborg, P. N. R. Vennestrøm, I. I. Ivanova, *J. Phys. Chem. Lett.* **2018**, *9*, 3738-3743; f) G. Qi, Q. Wang, J. Xu, Q. Wu, C. Wang, X. Zhao, X. Meng, F. Xiao, F. Deng, *Communications Chemistry* **2018**, *1*, 22; g) J. W. Harris, W.-C. Liao, J. R. Di Iorio, A. M. Henry, T.-C. Ong, A. Comas-Vives, C. Copéret, R. Gounder, *Chem. Mater.* **2017**, *29*, 8824-8837; h) P. Wolf, M. Valla, F. Núñez-Zarur, A. Comas-Vives, A. J. Rossini, C. Firth, H. Kallas, A. Lesage, L. Emsley, C. Copéret, I. Hermans, *ACS Catal.* **2016**, *6*, 4047-4063.

[11] M. Boronat, A. Corma, M. Renz, *J. Phys. Chem. B* **2006**, *110*, 21168-21174.

[12] R. Bermejo-Deval, M. Orazov, R. Gounder, S.-J. Hwang, M. E. Davis, *ACS Catal.* **2014**, *4*, 2288-2297.

[13] C. Hammond, D. Padovan, A. Al‐Nayili, P. P. Wells, E. K. Gibson, N. Dimitratos, *ChemCatChem* **2015**, *7*, 3322-3331.

[14] a) A. Corma, L. T. Nemeth, M. Renz, S. Valencia, *Nature* **2001**, *412*, 423-425; b) M. Renz, T. Blasco, A. Corma, V. Fornés, R. Jensen, L. Nemeth, *Chem. Eur. J.* **2002**, *8*, 4708-4717.

[15] a) M. Hunger, J. Weitkamp, *Angew. Chem. Int. Ed.* **2001**, *40*, 2954-2971; b) J. Xu, Q. Wang, F. Deng, *Acc. Chem. Res.* **2019**, *52*, 2179-2189; c) J. Xu, Q. Wang, S. Li, F. Deng, *Solid-State NMR in Zeolite Catalysis*, Springer, Singapore, **2019**.

[16] D. Klomp, T. Maschmeyer, U. Hanefeld, J. A. Peters, *Chem. Eur. J.* **2004**, *10*, 2088-2093.

[17] S. Lang, M. Benz, U. Obenaus, R. Himmelmann, M. Hunger, *ChemCatChem* **2016**, *8*, 2031-2036.

[18] W. Wang, M. Hunger, *Acc. Chem. Res.* **2008**, *41*, 895-904.

[19] J. March, *Advanced Organic Chemistry*, Wiley, New York, **1992**.

[20] A. F. Crespi, D. Vega, A. K. Chattah, G. A. Monti, G. Y. Buldain, J. M. Lázaro-Martínez, *J. Phys. Chem A* **2016**, *120*, 7778-7785.

[21] A. F. Crespi, A. J. Byrne, D. Vega, A. K. Chattah, G. A. Monti, J. M. Lázaro-Martínez, *J. Phys. Chem A* **2018**, *122*, 601-609.

[22] J. Xu, A. M. Zheng, X. M. Wang, G. D. Qi, J. H. Su, J. F. Du, Z. H. Gan, J. F. Wu, W. Wang, F. Deng, *Chem. Sci.* **2012**, *3*, 2932-2940.

[23] L. Chen, Q. Wang, B. Hu, O. Lafon, J. Trébosc, F. Deng, J.-P. Amoureux, *Phys. Chem. Chem. Phys.* **2010**, *12*, 9395-9405.

[24] A. V. Yakimov, Y. G. Kolyagin, S. Tolborg, P. N. R. Vennestrøm, I. I. Ivanova, *J. Phys. Chem. C* **2016**, *120*, 28083-28092.

[25] T. R. Josephson, G. R. Jenness, D. G. Vlachos, S. Caratzoulas, *Micropor. Mesopor. Mat.* **2017**, *245*, 45-50.

[26] a) A. J. Tasiopoulos, S. P. Perlepes, *Dalton Trans.* **2008**, 5537-5555; b) D. P. Giannopoulos, L. Cunha-Silva, R. Ballesteros-Garrido, R. Ballesteros, B. Abarca, A. Escuer, T. C. Stamatatos, *RSC Adv.* **2016**, *6*, 105969-105979.

[27] a) D. Klomp, T. Maschmeyer, U. Hanefeld, J. A. Peters, *Chem. Eur. J.* **2004**, *10*, 2088-2093; b) O. Pàmies, J.-E. Bäckvall, *Chem. Eur. J.* **2001**, *7*, 5052-5058.

[28] a) R. Cohen, C. R. Graves, S. T. Nguyen, J. M. L. Martin, M. A. Ratner, *J. Am. Chem. Soc.* **2004**, *126*, 14796-14803; b) R. S. Assary, L. A. Curtiss, J. A. Dumesic, *ACS Catal.* **2013**, *3*, 2694-2704; c) P. K. Agarwal, S. P. Webb, S. Hammes-Schiffer, *J. Am. Chem. Soc.* **2000**, *122*, 4803-4812.